A novel mechanism of inhibition by phenylthiourea on PvdP, a tyrosinase synthesizing pyoverdine of Pseudomonas aeruginosa

Wibowo, Joko P; Batista, Fernando A; van Oosterwijk, Niels; Groves, Matthew R; Dekker, Frank J; Quax, Wim J

Published in:
International Journal of Biological Macromolecules

DOI:
10.1016/j.ijbiomac.2019.12.252

Publication date:
2020

International Journal of Biological Macromolecules 146 (2020) 212–221

Contents lists available at ScienceDirect

International Journal of Biological Macromolecules

journal homepage: http://www.elsevier.com/locate/ijbiomac

A novel mechanism of inhibition by phenylthiourea on PvdP, a tyrosinase synthesizing pyoverdine of *Pseudomonas aeruginosa*

Joko P. Wibowo [a,b], Fernando A. Batista [c], Niels van Oosterwijk [c], Matthew R. Groves [c], Frank J. Dekker [a], Wim J. Quax [a,*]

[a] Department of Chemical and Pharmaceutical Biology, Groningen Research Institute of Pharmacy, University of Groningen, the Netherlands
[b] Faculty of Pharmacy, University of Muhammadiyah Banjarmasin, Banjarmasin, Indonesia
[c] Department of Drug Design, Groningen Research Institute of Pharmacy, University of Groningen, the Netherlands

ARTICLE INFO

Article history:
Received 4 October 2019
Received in revised form 6 December 2019
Accepted 28 December 2019
Available online 30 December 2019

Keywords:
Pseudomonas aeruginosa
Pyoverdine
PvdP
Tyrosinase
Phenylthiourea

ABSTRACT

The biosynthesis of pyoverdine, the major siderophore of *Pseudomonas aeruginosa*, is a well-organized process involving a discrete number of enzyme-catalyzed steps. The final step of this process involves the PvdP tyrosinase, which converts ferribactin into pyoverdine. Thus, inhibition of the PvdP tyrosinase activity provides an attractive strategy to interfere with siderophore synthesis to manage *P. aeruginosa* infections. Here, we report phenylthiourea as a non-competitive inhibitor of PvdP for which we solved a crystal structure in complex with PvdP. The crystal structure indicates that phenylthiourea binds to an allosteric binding site and thereby interferes with its tyrosinase activity. We further provide proofs that PvdP tyrosinase inhibition by phenylthiourea requires the C-terminal lid region. This provides opportunities to develop inhibitors that target the allosteric site, which seems to be confined to fluorescent pseudomonads, and not the tyrosinase active site. Furthermore, increases the chances to identify PvdP inhibitors that selectively interfere with siderophore synthesis.

1. Introduction

Nowadays, many bacteria have become resistant to multiple common antibiotics [1] by acquiring diverse resistance mechanisms [2]. Antibiotic resistance poses an increasing challenge to our healthcare system. Therefore, new strategies to develop novel antibiotics are urgently sought after. An alternative approach to design novel antibiotics is by depriving bacteria from their supply of essential metals like, for example iron. This metal acts as an essential cofactor in a number of bacterial enzymes and due to its limited supply it is one of the growth-limiting factors [3]. Iron levels in the human body are tightly controlled by many transport and storage mechanism thus leaving the free iron concentrations below 1 μM [4]. To overcome this problem, bacteria such as *Pseudomonas aeruginosa* secrete siderophores, which are high-affinity chelating molecules that can capture iron at very low molarity ($Kf \sim 10^{24}\ M^{-1}$) [5], allowing the bacterium to compete for iron binding with endogenous human iron binding proteins such as transferrin [6].

The major siderophore of *P. aeruginosa* is pyoverdine [7]. Pyoverdine binds ferric ion (Fe^{3+}) to form a ferripyoverdine complex that can be taken up via a specific receptor (FpvA) into the cell [8]. In the periplasm, the Fe^{3+} is released and converted into Fe^{2+} by FpvC and FpvF and taken up by FpvDE transporter into the cytoplasm [9]. Apart from iron binding, pyoverdine is known as a virulence factor that autoregulates the production of pyoverdine itself and also upregulates the production of PrpL protease and exotoxin A, which are two other major virulence factors of *P. aeruginosa* [10]. This key role indicates the potency to control infections caused by these bacteria through interfering with pyoverdine synthesis. Indeed, several studies demonstrated that *P. aeruginosa* pyoverdine-deficient mutants were not infectious [11,12].

The biosynthesis of pyoverdine involves at least 4 non-ribosomal peptide synthetases (NRPs) and 10 other enzymes located in the cytoplasm and the periplasm of *P. aeruginosa* [8]. In the final step of the biosynthesis, at least five enzymes are involved: PvdM, PvdN, PvdO, PvdP and PvdQ. A recent study reported that a biaryl nitrile compound, ML318, can inhibit PvdQ in vitro and in a bacterial cell assay [13]. PvdQ is an Ntn-hydrolase located in the periplasm, which is also involved in the biosynthesis of pyoverdine [14]. It means that the inhibition of pyoverdine biosynthesis through the inhibition of a pyoverdine synthesizing enzyme can lead to inhibition of virulence and infection.

* Corresponding author at: Department of Chemical and Pharmaceutical Biology, Groningen Research Institute of Pharmacy, University of Groningen, Antonius Deusinglaan 1, Groningen, 9713 AV, the Netherlands.
E-mail address: w.j.quax@rug.nl (W.J. Quax).

https://doi.org/10.1016/j.ijbiomac.2019.12.252

PvdP (EC 1.14.18.1) is known from its key role in the maturation of the pyoverdine chromophore [15]. In addition, it has been reported that a *P. aeruginosa* PvdP knock out mutant cannot produce pyoverdine anymore [16]. Therefore, it is reasonable to presume that inhibition of PvdP can block the production of pyoverdine. PvdP is a member of the tyrosinase super family, but shows limited structural homology to eukaryotic tyrosinases.

In this study, we aim to identify novel small molecule inhibitors of the PvdP tyrosinase by screening a collection of compounds that have been reported to inhibit other members of the tyrosinase super family. The screening provided phenylthiourea as a non-competitive inhibitor of PvdP tyrosinase and crystallographic analysis demonstrated phenylthiourea binding to an allosteric binding site of PvdP. Crystallographic analysis also revealed that PvdP has an unusual C-terminal lid structure covering the active site. The data show that phenylthiourea binding freezes the lid, thus interfering with enzymatic activity. Altogether, this indicates a novel mechanism to interfere selectively with PvdP tyrosinase activity.

2. Materials and methods

2.1. Cloning and expression of PvdP

The PvdP gene was PCR amplified and cloned from *P. aeruginosa* PA01 with additional N-terminal His·Tag® in pET-28a DNA-Novagen (Merck & Co., USA) using standard protocol. Then, the plasmid pET-28a-PvdP was transformed into *Escherichia coli* BL21 (DE3) competent cells. To produce the enzyme, we followed the published protocol with a minor modification [15]. Ten milliliter overnight preculture in LB media (~1.5×10^9 CFU/mL) was added into 1 L 2xTY media (both media supplemented with 50 μg/mL kanamycin). Enzyme expression was induced with 0.1 mM isopropyl 1-thio-β-D-galactopyranoside (IPTG) after OD_{600} of the culture reached 0.8 in a 200 rpm shaking incubator at 30 °C. After overnight incubation in a 200 rpm shaking incubator at 20 °C the bacterial cells were harvested by centrifugation for 15 min at 5000*g* (Sorvall™ RC6, Thermo Fisher Scientific, USA) at 4 °C.

2.2. Purification of PvdP

To purify the PvdP wildtype and PvdP without the C-terminal lid covering the active site (PvdP-trunc) enzymes, we followed the published protocol [15]. The final concentration was determined based on the protein absorbance at 280 nm. The estimated protein purity was higher than 95% assessed by Coomassie Brilliant Blue-stained SDS-PAGE [17]. The both enzymes were concentrated to 5 mg/mL in 20 mM TRIS-HCl pH 8.0 buffer, aliquoted, snap-frozen and stored in −80 °C until used for testing the compounds. For crystallization, the buffer was exchanged via size-exclusion chromatography using HiLoad 16/60 Superdex 75 column (GE Healthcare, USA) pre-equilibrated with gel-filtration buffer (10 mM MMT pH 8.0, 100 mM ammonium chloride). The purified enzyme eluted as a single peak and was pooled and concentrated to 10 mg/mL at 4 °C.

2.3. Screening of mushroom tyrosinase inhibitors against PvdP activity

Commercially available mushroom tyrosinase inhibitors (Fig. S1) were selected and their inhibitory activity on PvdP were determined. The selection was based on the availability, diverse scaffolds and their potency on mushroom tyrosinase. All chemical compounds were analytical grade.

The conversion of 0.5 mM of L-tyrosine to dopachrome (475 nm) by 25 μg PvdP in 1 mL of 50 mM CHES (pH 8.0) and 250 μM $CuSO_4$ in the presence of 200 μM (diluted in 5% DMSO) tested compound was monitored using an SPECTROstar® Omega microplate reader (BMG Labtech, Germany) on a 96 wells flat bottom transparent plate (VWR International, USA) for 30 min at 30 °C. The mixtures were incubated at 30 °C for 5 min prior to monitoring. The percentage inhibition of each compound was compared to the positive control which was determined using the same assay as mentioned above. The IC_{50} value of potential inhibitors was determined based on a dose response curve of the percent inhibition against PvdP. All of the measurements were done in triplicate.

2.4. Kinetic experiments with phenylthiourea

For the enzyme kinetic experiments, the reaction mixture consisted of the same components as mentioned above but using different concentration of substrate and inhibitor. We used substrate at concentration 0.1, 0.2, 0.3, 0.4, 0.5, 0.7, 1.0 and 1.5 mM. Concentrations of the inhibitor were arranged to comprise the IC_{50} value and analyzed through Lineweaver-Burk plots. The obtained data were plotted as 1/velocity (1/V) vs 1/substrate concentration (1/[S]) based on Lineweaver-Burk plots. The Michaelis-Menten constant (K_m) and maximum velocity (V_{max}) were also determined under the same reaction mixture.

2.5. Activity of phenylthiourea on PvdP-trunc

In order to measure the activity of the inhibitor on PvdP-trunc, a set of reaction mixture as mentioned above was prepared. Phenylthiourea 300 μM was incubated in the mixture for 5 min prior to addition of substrate and measurement. We used PvdP wildtype as a control using the same concentration of phenylthiourea.

2.6. Buffer screening for crystallization of PvdP

In order to select the correct buffer for crystallization, a thermofluor-based stability assay was performed [18,19]. We used SYPRO® Orange dye (Invitrogen, USA) and followed a protocol by Lunev to perform the assay [20].

2.7. Crystallization of PvdP bound to copper (PvdP-Cu) and PvdP bound to copper and phenylthiourea (PvdP-Cu-PTU)

Screening for crystallization conditions for PvdP was performed using a high throughput crystallization robot Crystal Gryphon (Art Robbins Instrument, USA) and commercially available sparse-matrix screening kits JCSG-*plus*™ and PACT *premier*™ (Molecular Dimensions, UK). All experiments were performed at 18 °C using the sitting drop vapour diffusion technique in 96-well MRC plates (Molecular Dimensions, UK). Equal volumes (0.3 μL) of protein solution and crystallization reagent were equilibrated in 50 μL of reservoir solution. Medium size single crystals appeared within 7 days in various drops containing Bis-Tris propane and PEG 3350. Further optimization was performed by varying the precipitant concentration and the pH. The optimal condition of the crystallization consists of equal amount (1 μL) of 10 mg/mL PvdP and 20% (w/v) PEG 3350 in 0.1 M Bis-Tris Propane pH 7.5 at 18 °C. The PvdP-Cu and PvdP-Cu-PTU crystals also grew within 7 days in the optimal condition mentioned above with the addition of 500 μM $CuSO_4$ and 500 μM $CuSO_4$ with 1 mM phenylthiourea, respectively.

2.8. Diffraction data collection and processing

PvdP crystals were harvested using mounted LythoLoops (Molecular Dimensions, UK), transferred to cryo-buffer and subsequently flash-frozen in −196 °C liquid nitrogen. The cryo-buffer was chosen based on the estimation from Garman & Mitchell [21] and consisted of 20% (w/v) PEG 3350 and 25% (v/v) glycerol in 0.1 M Bis-Tris Propane pH 7.5. The x-ray diffraction data were collected at −173 °C at the P11 beamline of the Deutsches Elektronen-Synchrotron (Hamburg, Germany). The intensity data were processed and scaled with XDS

[25] and Aimless [22] from the CCP4 package [23]. An overview of the data collection statistics can be found in Table 1.

2.9. Phasing and refinement

The structure of PvdP was solved using a SAD dataset collected from a selenomethionine labelled crystal. An X-ray fluorescence wavelength scan was performed and the result was analyzed using CHOOCH. A clear peak for selenium was detected and a SAD dataset was collected at the derived peak wavelength. The autosol wizard [24] from the PHENIX package [25] could solve the structure and subsequently auto-build around 80% of the residues in the structure (R/Rfree = 28/36). After several cycles of manual model building using COOT [26] combined with phased refinement using non-crystallographic symmetry (NCS) restraints for all four molecules in the asymmetric unit using Refmac5 [27] the initial model of obtained from the selenomethionine data was transferred to the native data set using PHASER [28], where the model building and refinement was completed. The refined structure of apo-PvdP was used to solve the structure of the PvdP-Cu and PvdP-Cu-PTU by molecular replacement.

The quality of the final models and the geometrical restraints were checked using Molprobity [29]. The coordinates and structure factor amplitudes have been deposited in the Protein Data Bank with accession codes 6RRR (PvdP), 6RRQ (PvdP-Cu) and 6RRP (PvdP-Cu-PTU). Figures of the structures were created using PyMOL 2.0.7 [30].

Table 1
X-ray data collection and refinement statistics.

	Semet PvdP	PvdP	PvdP-Cu	PvdP-Cu-PTU
PDB ID	–	6RRR	6RRQ	6RRP
Data collection				
Space group	$P12_11$	$P12_11$	$P12_11$	$P12_11$
Cell dimensions				
a, b, c (Å)	93.20, 107.62, 108.30	44.16, 112.62, 100.26	50.72, 114.22, 100.91	50.239 113.88 100.577
α, β, γ (°)	90.00, 98,79, 90.00	90.00, 92,71, 90.00	90.00, 94.82, 90.00	90 94.335 90
Wavelength (Å)	1.033200	1.033200	1.033200	1.033200
Resolution (Å)	50.00–2.50	45.76–2.11	46.22–2.70	49.52–2.40
R_{merge} (%)		8.16 (74.52)	14.9 (10.01)	7.6 (58.1)
⟨I/σ (I)⟩		13.01 (1.98)	11.97 (1.79)	10.81 (1.97)
Completeness	93.47	99.36 (97.22)	99,25 (99.02)	99.66 (98.86)
Multiplicity		4.5 (4.5)	3.7 (3.6)	3.8 (3.8)
Refinement				
Resolution (Å)		45.76–2.11	46.22–2.70	49.52–2.40
No. of reflections		55,908 (5420)	31,331 (3143)	43,995 (4351)
R_{work}/R_{free} (%)		17.17/21.93	19.51/25.39	20.11/25.47
No. of atoms				
Protein		7641	7317	7465
Ligand/ion		12	10	24
Water		508	131	211
B-factors (Å)				
Protein		35.22	50.69	47.95
Ligand/ion		48.93	52.68	77.25
Water		35.13	34.80	39.99
R.m.s. deviations				
Bond lengths (Å)		0.014	0.011	0.016
Bond angles (°)		1.76	1.47	1.93

3. Results and discussions

3.1. Inhibitory activity of the selected mushroom tyrosinase inhibitors on PvdP

In this study we aim to identify small molecule inhibitors of the PvdP tyrosinase activity as a potential novel therapeutic option for the treatment of bacterial infection caused by *P. aeruginosa*. To achieve this aim, we tested mushroom tyrosine inhibitors on the enzymatic activity of PvdP, because mushroom tyrosinase is one of the most investigated tyrosinases. Moreover, many inhibitors for mushroom tyrosinase have been reported [31]. Screening of the collection of mushroom tyrosinase inhibitors shows that some compounds inhibit PvdP tyrosinase activity in a concentration-dependent manner. The inhibitory concentration 50% (IC_{50}) values of those compounds were determined (Table 2).

Kojic acid is often used as reference compound and it inhibits mushroom tyrosinase with micromolar potency. However, for PvdP tyrosine activity the potency is proven to be limited to the high micromolar range (IC_{50} = 0.75 ± 0.04 mM). Surprisingly, the other inhibitor, l-mimosine, showed no inhibition on the enzymatic activity of PvdP. Tropolone, kuraridin and piceatannol, which are stronger inhibitors on the mushroom tyrosinase than kojic acid, also showed no inhibition on PvdP. Similarly, the weak inhibitors of mushroom tyrosinase (stigmasterol, morin hydrate, naringin) also showed no inhibition. It gave an early indication that PvdP is a unique tyrosinase among the other tyrosinases. Interestingly, among the tested compounds, phenylthiourea, a sulfur-containing compound proved to be the most potent inhibitor of PvdP in this series (IC_{50} = 174.4 ± 8.9 μM).

3.2. Kinetic experiments with phenylthiourea

Enzyme kinetics experiments for the inhibition of PvdP tyrosinase activity by phenylthiourea were performed in order to characterize the binding further. The K_m value for L-tyrosine, which was employed as a substrate, proved to be 1.36 mM, which was comparable to previously reported values [15]. The results of the non-linear curve fitting showed that phenylthiourea did not change the K_m values of PvdP towards its substrate L-tyrosine. However, a reduction of V_{max} values was observed by increasing the phenylthiourea concentration (Fig. 1A). The type of inhibition was then confirmed by double reciprocal Lineweaver-Burk plots in the presence of different concentration of phenylthiourea. The Lineweaver-Burk plots clearly indicated phenylthiourea as a non-competitive inhibitor (Fig. 1B). This information also gave another indication that PvdP is different from other tyrosinases. Because on the previous reports phenylthiourea has been reported as a competitive inhibitor of mushroom tyrosinase (IC_{50} = 0.55 ± 0.07 μM) [32] and sweet potato tyrosinase (IC_{50} = 43 μM) [33].

Table 2
Quantitative inhibitory activity of mushroom tyrosinase inhibitors against PvdP and mushroom tyrosinase (IC_{50} ± SD in μM).

Compounds	PvdP	Mushroom tyrosinase (based on references)
Kojic acid	750 ± 43	16.67 ± 0.52 [33]
Tropolone	>1000	1.2 [34]
Phenylthiourea	174.4 ± 8.9	0.55 ± 0.07 [35]
Stigmasterol	N.I.	N.I. [33]
L-mimosine	N.I.	3.68 ± 0.02 [33]
Morin hydrate	N.I.	81.3 ± 12.1 [36]
Kuraridine	N.I.	0.6 [37]
Sesamol	N.I.	1.6 [38]
Naringin	N.I.	>1000 [39]
Piceatannol	N.I.	1.53 [40]
Quercetine	N.I.	>1000 [41]

N.I. = no inhibition; SD = standard deviation.

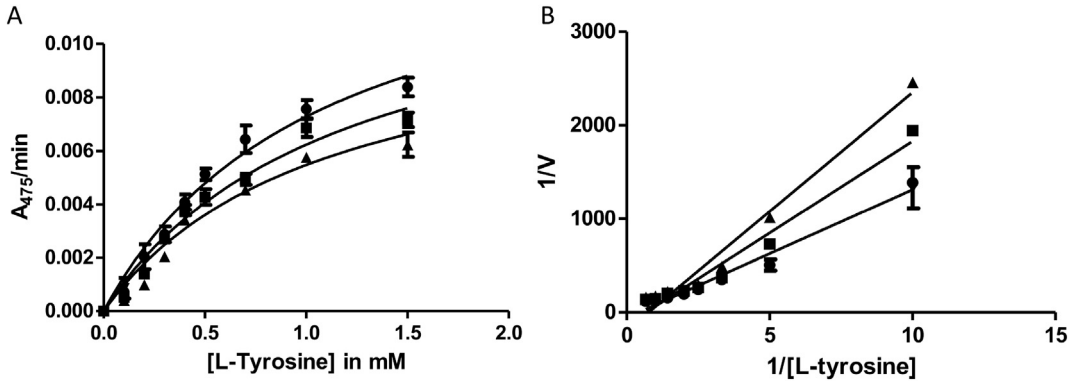

Fig. 1. The kinetic studies of phenylthiourea inhibitory activity on PvdP. (A) Michaelis-Menten; and (B) Lineweaver-Burk plots. The lines with circle, square and triangle symbol correspond to the concentrations of phenylthiourea at 0, 50, 100 μM, respectively. Data were presented as mean ± SD (n = 3).

3.3. Crystal structure of PvdP, PvdP-Cu and PvdP-Cu-PTU

In this paper, we reported the structure of apo-PvdP solved by the single-wavelength anomalous diffraction (SAD) method of selenomethionine labelled PvdP (Semet PvdP). The structure of apo-PvdP has been solved independently [34]. The two apo structures are similar and refined to 2.1 Å resolution.

PvdP is known as a copper dependent enzyme [15]. Therefore, to get insight of its active state at the molecular level, we co-crystallized PvdP in the presence of Cu^{2+}. In addition, to understand the interaction between phenylthiourea and PvdP, we did a co-crystallization of PvdP with Cu^{2+} and phenylthiourea. The structure PvdP bound to Cu (PvdP-Cu) and PvdP bound to Cu^{2+} and phenylthiourea (PvdP-Cu-PTU) were solved by molecular replacement (MR) of the apo structure to 2.7 Å and 2.4 Å resolution, respectively. The two latter structures are novel and they provide interesting insight in the enzymatic mechanism as discuss below. The structure of PvdP (6RRR), PvdP-Cu (6RRQ) and PvdP-Cu-PTU (6RRP) has been deposited to the Protein Data Bank. All of the PvdP crystals belong to space group P21 and were confirmed to have two molecules in the asymmetry unit. The overall model structures are in good quality as they have R and R_{free} factors below 0,27.

A comparison of the crystal structure of PvdP (PDB ID = 6RRR) and other tyrosinases also supported the facts above. Based on the sequence alignment analysis (Clustal Omega, https://www.ebi.ac.uk/Tools), PvdP is very distinct from other tyrosinases. The closest homolog of PvdP is tyrosinase of *Bacillus megaterium* (PDB ID = 3NQ5) having sequence

Table 3
Tyrosinase structure comparison.

No	Tyrosinase	Metal	Inhibitor	PDB	Lid covering active site
1	*Agaricus bisporus*	Cu	–	2Y9X	No
2	*A. bisporus*	Cu	Tropolone	2Y9W	No
3	*Homo sapiens*	Zn	–	5M8L	No
4	*H. sapiens*	Zn	Tropolone	5M8O	No
5	*H. sapiens*	Zn	Kojic acid	5M8M	No
6	*H. sapiens*	Zn	Phenylthiourea	5M8S	No
7	*Bacillus megaterium*	Cu	–	3NPY	No
8	*B. megaterium*	Cu	Kojic acid[a]	3NQ1	No
9	*B. megaterium*	Cu	SVF	5OAE	No
10	*B. megaterium*	Cu	Kojic acid[b]	5I38	No
11	*B. megaterium*	Cu	p-Tyrosol	4P6T	No
12	*Juglans regia*	Cu	–	5CE9	No
13	*Streptomyces castaneoglobisporus*	Cu	–	1WXC	No
14	*P. aeruginosa*	Zn	–	6EYV	No
15	*P. aeruginosa*	–	–	6EYS	Yes
16	*P. aeruginosa*	Cu	–	6RRQ	No
17	*P. aeruginosa*	Cu	Phenylthiourea	6RRP	Yes

[a] Kojic acid bound not in the active site.
[b] Kojic acid bound in the active site.

identity of only 30,77%. Further investigation showed that PvdP is the only tyrosinase with a C-terminal lid covering the active site while the other tyrosinases do not have this lid (Table 3).

3.4. Structural analysis of PvdP structures

The crystal structure of apo-PvdP showed no copper-binding in the active sites but putative binding sites were occupied by water molecules. The active site is covered by a unique C-terminal lid with Tyr531 residue blocking the substrate-binding pocket (Fig. 2A). The crystal structure of PvdP-Cu clearly shows the presence of two Cu^{2+} ions (CuA and CuB) in the active site. This structure differs from the previously published structure (PDB ID = 6EYV) since they have Zn^{2+} ions in the active site instead of Cu^{2+}. The CuA is tetrahedrally coordinated with His216, His220, His271 and CuB with His375, His379, and His432. The distance between the two Cu^{2+} ions is 4.1 Å. This structure shows that the C-terminal lid is non-visible suggesting a random orientation of the lid, which means that the active site is opened in the presence of Cu^{2+} (Fig. 2B). This opening is due to displacement rather than to proteolytic cleavage. This is confirmed by a LC-MS analysis where the two enzyme conformations are shown to have the similar molecular weight (Fig. S2). Apparently, this structural rearrangement has major consequences to the PvdP crystal, since the mature and relatively big size apo crystals were destroyed immediately when we soaked them with $CuSO_4$.

This information is in concert with the observation that the presence of Cu^{2+} ions is essential for the activity of PvdP [15]. It suggests a mechanism in which opening of the lid in the presence of Cu^{2+} giving an access to the substrate to reach the active site. This control of access to the active side facilitated by Cu^{2+} ions has not been reported on the other tyrosinase structures that have been published.

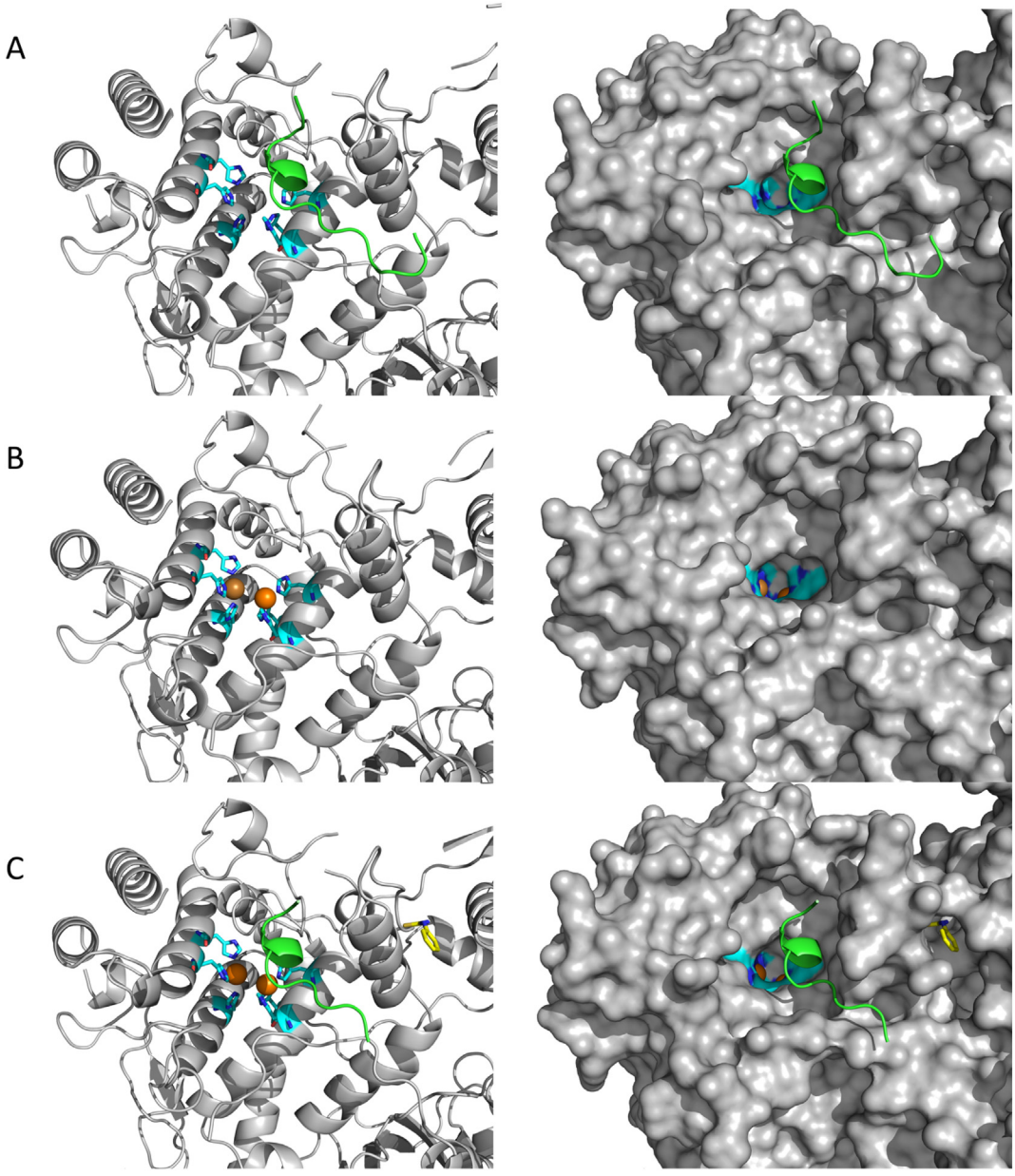

Fig. 2. Comparison of the C-terminal lid among all of PvdP structures. (A) Crystal structure of apo PvdP (PDB ID = 6RRR), the C-terminal lid is present (green cartoon) (B) Crystal structure of PvdP-Cu (PDB ID = 6RRQ), the C-terminal lid is invisible in the presence of copper (orange sphere) and (C) Crystal structure of PvdP-Cu-PTU (PDB ID = 6RRP), the C-terminal lid is present again (green cartoon) together with copper ions in the active site (orange spheres). The six histidine residues of the active site are depicted in cyan, phenylthiourea is depicted in yellow. All figures were prepared with PyMOL 2.0.7 [30].

The crystal structure PvdP-Cu-PTU gave us more insight into the inhibition mechanism of phenylthiourea on PvdP (Fig. 2C). In this structure, strong electron density is found in the active site, which corresponds to the binding of copper ions at the expected locations in the active site. In addition, phenylthiourea displays strong electron density in the binding pocket at the interface between the C-terminal domain and the N-terminal domain (Fig. 3A). It locates close to the end part of the C-terminal lid covering the active site. Structural analysis indicates the presence of hydrogen bonding and hydrophobic interactions between phenylthiourea and the surrounding residues. The thioketone group of phenylthiourea has two interactions with Trp320 and Ser329 at a distance of 3.1 Å and 2.8 Å, respectively. The NH group is in a distance of 3.4 Å to Arg53 and the NH_2 group is slightly closer to His333 at 3.2 Å (Fig. 3B). A structure comparison between apo PvdP and PvdP-Cu-PTU structures indicates a very subtle rotation of the beta-barrel domain towards the tyrosinase domain in each of the two monomers upon binding of phenylthiourea.

The residues are part of the interface between the N-terminal β-barrel domain (BBD) and the C-terminal tyrosinase domain (TYD) of PvdP. This interface is mostly composed of helices α9, α10 and linker sequences (residues 292–299) on the TYD site and a large portion of the BBD domain. Five H-bonds stabilize the interface: one between Asp56 and His333, one between Asp86 and Leu297 and three being formed from Arg301 bridging to Leu104, Ala106, and Glu108 (Fig. 4A). The binding of phenylthiourea to this interface increases its stability by increasing the number of interactions, with three anchor points on the TYD (Trp320, Ser329 and His333) and one on BBD (Arg53) (Fig. 4B). Analysis of the B-factors revealed a decreased vibration motion of helix α10, from which Trp320, Ser329 and His333 are part of, when the PTU-bound structure was compared to both apo and Cu-bound structures (B-factor averages of 34.5, 47.8 and 48.4 respectively). Similarly, helix α1, from which Arg53 is part of, presented a lower degree of mobility (B-factors of 31.6, 41.6 and 43.6 for PTU-bound, apo and Cu-bound respectively). A decreased vibration motion was also observed in other regions of PTU-bound structure, including the active site (B-factor average of 26.9 against 38.3 for apo and 41.5 for Cu-bound structures). The comparison of B-factor averages of the complete structures revealed values of 32.7, 46.3 and 49.4 for PTU-bound, apo and Cu-bound structures respectively. This indicates that the binding of phenylthiourea to the interface between the two domains of PvdP reduces the

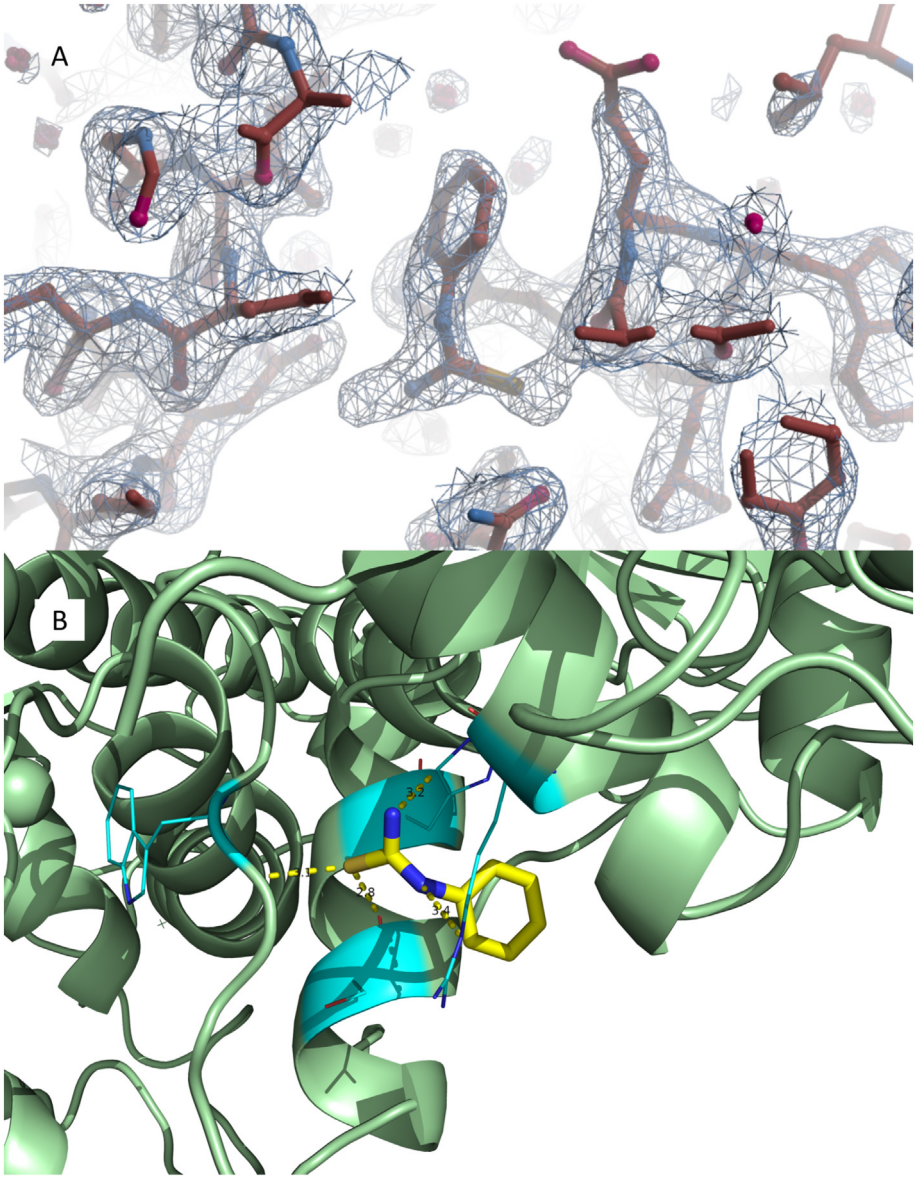

Fig. 3. Interaction of phenylthiourea with PvdP. (A) Representative 2Fo-Fc electron density of phenylthiourea is located in the interface between N-terminal domain and C-terminal domain, (B) phenylthiourea interacts with Arg53, Trp320, Ser329 and His333.

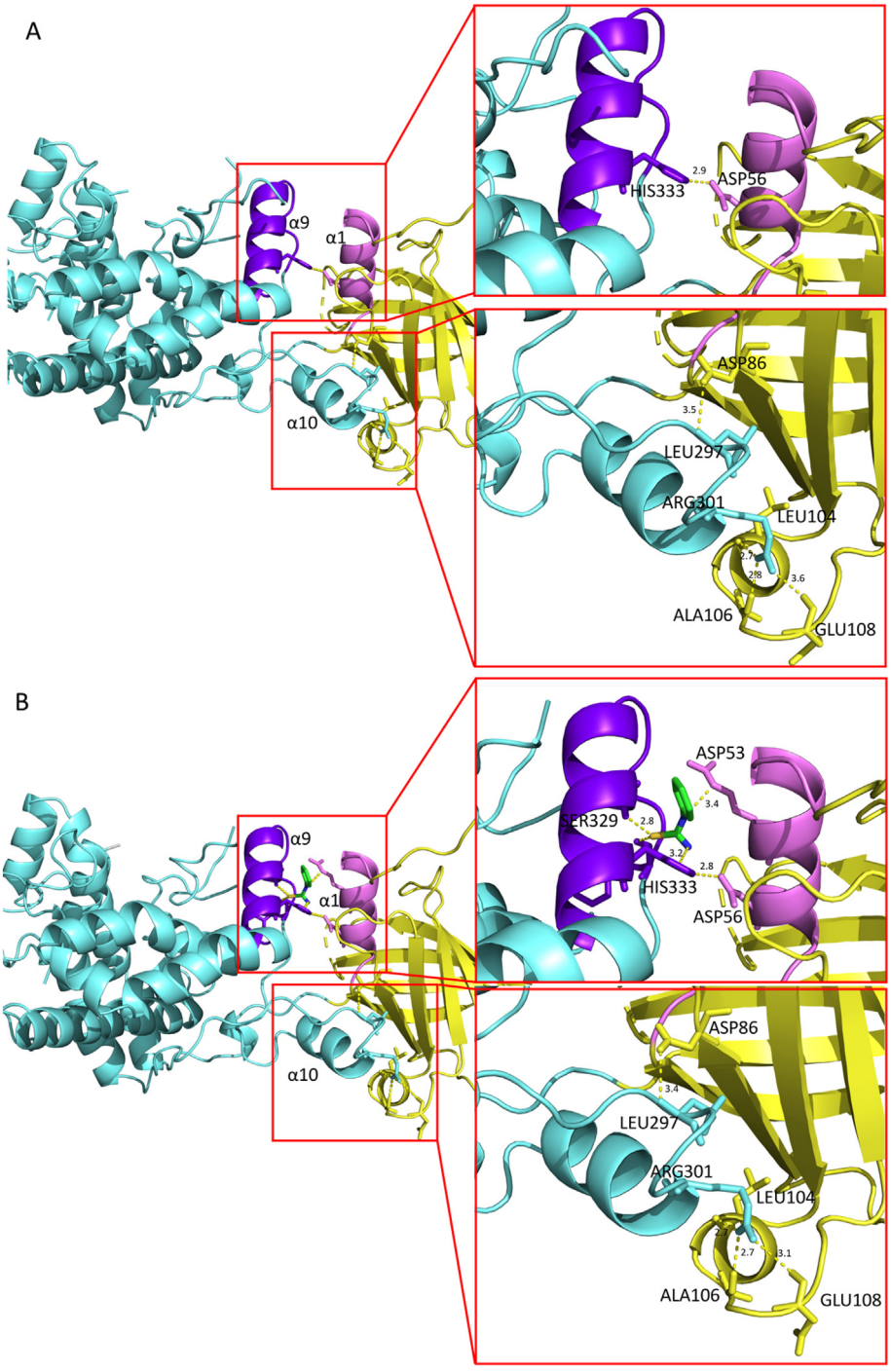

Fig. 4. A comparison structures of apo and Cu-PTU bound. (A) Apo PvdP structure has 5 H-bonds between TYD and BBD (B) the binding of phenylthiourea on PvdP increases interaction between two domains, three anchor points on TYD (Trp320, Ser329, His333) and one anchor point on BBD (Arg53).

overall mobility of the protein, resulting in a moderate inhibition of its tyrosinase activity by a novel allosteric mechanism.

Further structural analysis among PvdP and the other tyrosinase structures showed interesting facts. The interface was not found in the other tyrosinase structures and those residues are not conserved among the other tyrosinases (Fig. S3). This is a new mode of binding of a ligand to a tyrosinase, since the published structure of human tyrosinase (PDB ID = 5M8S) [35] and sweet potato tyrosinase (PDB ID = 1BUG) [36] show phenylthiourea binding in the active site.

Interestingly, the C-terminal lid that is open in the PvdP-Cu structure proves to be closed in the structure PvdP-Cu-PTU. As seen in our structures, the presence of phenylthiourea causes an ordering of C-terminal lid covering the active site. The binding of phenylthiourea promotes closing of the lid onto the PvdP active site. Presumably, due to phenylthiourea binding the lid opening is somehow distorted and comes back to its original position as observed in the apo-PvdP crystal structure. This lid prevents access of the substrate to the active site and, as a result, implies that phenylthiourea acts as an allosteric inhibitor of PvdP. Notably, the observed electron density of the lid in the PvdP-Cu-PTU structure is not as strong as in the apo-PvdP structure, but it clearly shows that the lid closes back onto the active site. Taken together, we observed that binding of phenylthiourea promotes closure of the lid even though the copper ions are present in the active site. This explains that phenylthiourea acts as an inhibitor that limits the access of the

substrate to the active site by binding to the lid structure, a mechanism well in line with non-competitive inhibition.

3.5. Inhibition mechanism of phenylthiourea on PvdP

To test this hypothesis, a mutant of PvdP without C-terminal lid denoted PvdP-trunc, was made to investigate the role of the C-terminal lid in the mechanism of inhibition of PvdP by phenylthiourea. To obtain this mutant, thirty-two amino acid residues of the C-terminal lid were deleted. The mutation did not change the enzyme kinetic properties the tyrosinase activity of PvdP. The K_m and V_{max} values of the mutant were determined under the same condition as for the native PvdP and showed no significant difference between them (Table S1). This strongly suggests that the residues of this lid are not involved in the catalytic activity.

The enzymatic activity of the mutant in the presence or absence phenylthiourea was investigated. In support of our hypothesis phenylthiourea acts as an inhibitor by binding to and stabilizing this lid, the assays demonstrated that phenylthiourea was unable to inhibit the activity of PvdP-trunc. Indeed, the addition of phenylthiourea up to 300 μM to the enzymatic assay did not influence the activity of the mutant (Fig. 5). In further support of the allosteric binding effect of phenylthiourea on PvdP, we show that kojic acid, which is known to bind to the mushroom tyrosinase active site, is able to inhibit both PvdP wildtype and PvdP-trunc at equivalent levels (data not shown). The results indicate that phenylthiourea inhibits PvdP wildtype but does not inhibit the truncated PvdP. This supports the hypothesis that the C-terminal lid is important for phenylthiourea mediated inhibition of PvdP tyrosinase activity. The presence of the C-terminal lid in the PvdP-Cu-PTU crystal structure regardless the presence of copper, and the activity of the lid-truncated PvdP in the presence of phenylthiourea provides to our opinion strong evidence that phenylthiourea actually decreases the terminal lid flexibility and consequently inhibits PvdP tyrosinase activity.

Considering the importance of pyoverdine as iron transporter into the bacterial cell, this system clearly represents a valuable therapeutic target. Several studies to develop anti-virulence agents against *P. aeruginosa* have been reported by targeting pyoverdine production [37–39]. A study reported inhibition on PvdQ, a Ntn-hydrolase involved in the biosynthesis pyoverdine, by small molecules showing inhibition of pyoverdine production in the bacterial cell assay up to micromolar range [13]. Another recent study reported that some compounds directly interact with pyoverdine thus reducing its pathogenicity and improving the survival of *Caenorhabditis elegans* after infection with *P. aeruginosa* [40]. Our finding indicates alternative strategy to develop anti-virulent by targeting PvdP as a new approach in the same pathway.

3.6. Docking simulation between ferribactin and PvdP

The docking results showed the ferribactin bound to PvdP in the active site and the tyrosine residue of ferribactin deeply buried in a distance 4.4 and 4.6 Å to the di-copper center (Fig. 6). Hydrogen interactions between the ligand and the residues, to be found alongside the ferribactin structure, stretch between 2.8 and 3.5 Å (Table S2). The predicted binding affinities is in a range between −7.1 and −6.3 kcal/mol (Table S3) in 9 possible poses. This docking result gives us more information about "open-close" mechanism of the active site via C-terminal lid movement. Ferribactin is a large substrate in size, in physiological condition, this mechanism guarantees ferribactin to be able to reach and bind to the active site.

4. Conclusions

Based on our results, PvdP has a distinct structural architecture compared to the other tyrosinases. PvdP has two domains (N-terminal and C-terminal domain) and a special C-terminal lid covering the active site. Phenylthiourea shows a non-competitive inhibitory activity through rearrangement of the C-terminal lid. The discovery that PvdP can be inhibited by non-competitive binding opens the possibility to develop a specific compound against *P. aeruginosa* infection, that will not inhibit other tyrosinases including human tyrosinases. Further optimization of drugs that exclusively inhibit the PvdP would be valuable.

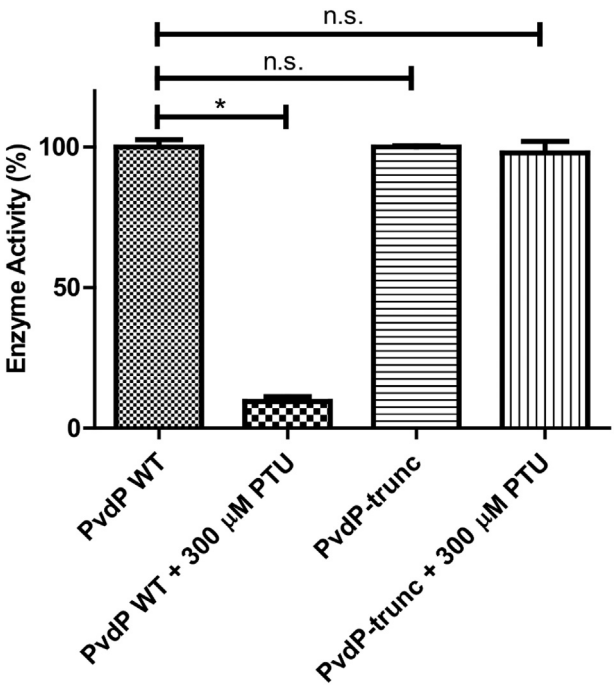

Fig. 5. Inhibition activity of 300 μM phenylthiourea on PvdP WT (wildtype) and PvdP-trunc. An asterisk (*) indicates significant difference and n.s. indicates non-significant difference between two groups ($P < 0.05$, Student's *t*-test). Data were presented as mean ± SD ($n = 3$).

CRediT authorship contribution statement

Joko P. Wibowo: Investigation, Data curation, Visualization, Writing - original draft, Funding acquisition.**Fernando A. Batista:**Investigation, Data curation, Visualization, Writing - original draft, Funding acquisition.**Niels van Oosterwijk:**Investigation, Data curation, Writing - original draft.**Matthew R. Groves:**Supervision, Resources, Writing - review & editing.**Frank J. Dekker:**Conceptualization, Supervision, Resources, Writing - review & editing.**Wim J. Quax:**Conceptualization, Supervision, Resources, Writing - review & editing.

Acknowledgements

The authors acknowledge to the staff at DESY III, Hamburg, Germany for providing access to the synchrotron radiation. The authors are grateful to Dr. Pol Nadal-Jimenez for making the construct of PvdP. Joko P. Wibowo is financially supported by Indonesia Endowment Fund for Education (Grant No. PRJ-418/LPDP/2016). Fernando A. Batista is supported by a funding through Science without Borders Fellowship from Conselho Nacional de Desenvolvimento Científico e Tecnológico (CNPq).

Database

RCSB Protein Data Bank ID: 6RRP, 6RRQ and 6RRR.

Funding

This work was supported by the Indonesia Endowment Fund for Education (Grant No. PRJ-418/LPDP/2016) and Science without Borders Fellowship from Conselho Nacional de Desenvolvimento Científico e Tecnológico (CNPq).

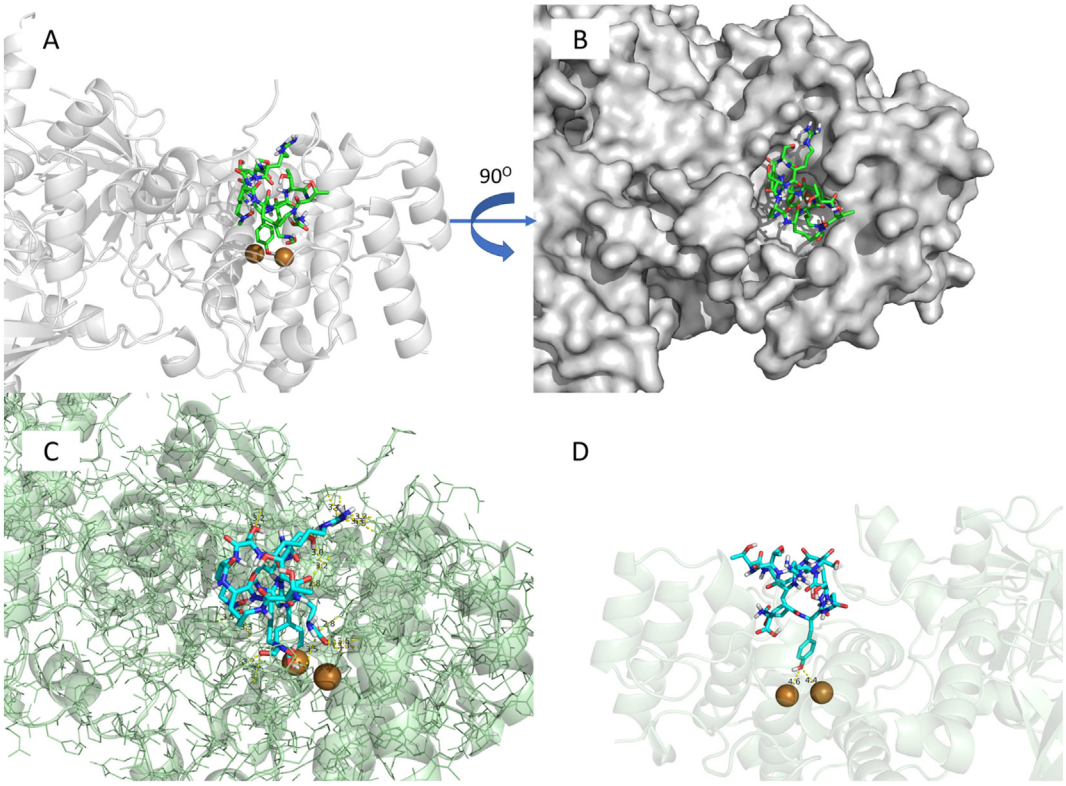

Fig. 6. Result of docking simulation between ferribactin and PvdP. (A) Front view and (B) top view show ferribactin located in the active site of PvdP. (C) Several hydrogen bonds between ferribactin and residues of PvdP. (D) Tyrosine residue of ferribactin is in the di-copper center at distance 4.4 and 4.6 Å.

Declaration of competing interest

The authors declare no conflict of interest.

Appendix A. Supplementary data

Supplementary data to this article can be found online at https://doi.org/10.1016/j.ijbiomac.2019.12.252.

References

[1] E. Geisinger, R.R. Isberg, Interplay between antibiotic resistance and virulence, J. Infect. Dis. 215 (2017) S9–S17, https://doi.org/10.1093/infdis/jiw402.
[2] J.M. Munita, C.A. Arias, Mechanisms of antibiotic resistance, Microbiol. Spectr. 4 (2016) 1–24, https://doi.org/10.1128/microbiolspec.VMBF-0016-2015.
[3] C. Ratledge, L.G. Dover, Iron metabolism in pathogenic bacteria, Annu. Rev. Microbiol. 54 (2000) 881–941, https://doi.org/10.1146/annurev.micro.54.1.881.
[4] G.O. Latunde-Dada, R.J. Simpson, Regulation of iron absorption and distribution, in: S. Yehuda, D.I. Mostofsky (Eds.), Iron Defic. Overload, Humana Press 2010, pp. 31–49, https://doi.org/10.1007/978-1-59745-462-9.
[5] P. Visca, F. Imperi, I.L. Lamont, Pyoverdine siderophores: from biogenesis to biosignificance, Trends Microbiol. 15 (2007) 22–30, https://doi.org/10.1016/j.tim.2006.11.004.
[6] S. Sriyosachati, C.D. Cox, Siderophore-mediated Iron Acquisition From Transferrin by Pseudomonas aeruginosa, 1986 doi:0019-9567/86/060885-07$02.00/0.
[7] C.D. Cox, P. Adams, Siderophore activity of pyoverdin for Pseudomonas aeruginosa, Infect. Immun. 48 (1985) 130–138doi:0019-9567/85/040130-09$02.00/0.
[8] I.J. Schalk, L. Guillon, Pyoverdine biosynthesis and secretion in Pseudomonas aeruginosa: implications for metal homeostasis, Environ. Microbiol. 15 (2013) 1661–1673, https://doi.org/10.1111/1462-2920.12013.
[9] G. Ganne, K. Brillet, B. Basta, B. Roche, F. Oise Hoegy, V.V. Gasser, I.J. Schalk, Iron release from the siderophore pyoverdine in Pseudomonas aeruginosa involves three new actors: FpvC, FpvG, and FpvH, ACS Chem. Biol. 12 (2017) 1056–1065, https://doi.org/10.1021/acschembio.6b01077.
[10] I.L. Lamont, P.A. Beare, U. Ochsner, A.I. Vasil, M.L. Vasil, S. Kustu, Siderophore-mediated signaling regulates virulence factor production in Pseudomonas aeruginosa, Proc. Natl. Acad. Sci. U. S. A. 99 (2002) 7072–7077, https://doi.org/10.1073/pnas.092016999.
[11] E. Papaioannou, M. Wahjudi, P. Nadal-Jimenez, G. Koch, R. Setroikromo, W.J. Quax, Quorum-quenching acylase reduces the virulence of Pseudomonas aeruginosa in a Caenorhabditis elegans infection model, Antimicrob. Agents Chemother. 53 (2009) 4891–4897, https://doi.org/10.1128/AAC.00380-09.
[12] F. Taguchi, T. Suzuki, Y. Inagaki, K. Toyoda, T. Shiraishi, Y. Ichinose, The siderophore pyoverdine of Pseudomonas syringae pv. tabaci 6605 is an intrinsic virulence factor in host tobacco infection, J. Bacteriol. 192 (2010) 117–126, https://doi.org/10.1128/JB.00689-09.
[13] J.M. Wurst, E.J. Drake, J.R. Theriault, I.T. Jewett, L. Verplank, J.R. Perez, S. Dandapani, M. Palmer, S.M. Moskowitz, S.L. Schreiber, B. Munoz, A.M. Gulick, Identification of inhibitors of PvdQ, an enzyme involved in the synthesis of the siderophore pyoverdine, ACS Chem. Biol. 9 (2014) 1536–1544, https://doi.org/10.1021/cb5001586.
[14] M. Bokhove, P.N. Jimenez, W.J. Quax, B.W. Dijkstra, The quorum-quenching N-acyl homoserine lactone acylase PvdQ is an Ntn-hydrolase with an unusual substrate-binding pocket, Proc. Natl. Acad. Sci. 107 (2009) 686–691, https://doi.org/10.1073/pnas.0911839107.
[15] P. Nadal-Jimenez, G. Koch, C.R. Reis, R. Muntendam, H. Raj, C. Margot Jeronimus-Stratingh, R.H. Cool, W.J. Quax, PvdP is a tyrosinase that drives maturation of the pyoverdine chromophore in Pseudomonas aeruginosa, J. Bacteriol. 196 (2014) 2681–2690, https://doi.org/10.1128/JB.01376-13.
[16] E. Yeterian, L.W. Martin, L. Guillon, L. Journet, I.L. Lamont, I.J. Schalk, Synthesis of the siderophore pyoverdine in Pseudomonas aeruginosa involves a periplasmic maturation, Amino Acids 38 (2010) 1447–1459, https://doi.org/10.1007/s00726-009-0358-0.
[17] U.K. Laemmli, Cleavage of structural proteins during the assembly of the head of bacteriophage T4, Nature 227 (1970) 680–685, https://doi.org/10.1038/227680a0.
[18] J.E. Nettleship, J. Brown, M.R. Groves, A. Geerlof, Methods for protein characterization by mass spectrometry, thermal shift (ThermoFluor) assay, and multiangle or static light scattering, in: B. Kobe, M. Guss, T. Huber (Eds.), Struct. Proteomics. Methods Mol. Biol, Humana Press 2008, pp. 299–318, https://doi.org/10.1007/978-1-60327-058-8_19.
[19] U.B. Ericsson, B.M. Hallberg, G.T. DeTitta, N. Dekker, P. Nordlund, Thermofluor-based high-throughput stability optimization of proteins for structural studies, Anal. Biochem. 357 (2006) 289–298, https://doi.org/10.1016/j.ab.2006.07.027.
[20] S. Lunev, S.S. Bosch, F.D.A. Batista, C. Wrenger, M.R. Groves, Crystal structure of truncated aspartate transcarbamoylase from Plasmodium falciparum, Acta Crystallogr. Sect. F Struct. Biol. Commun. F72 (2016) 523–533, https://doi.org/10.1107/S2053230X16008475.
[21] E.F. Garman, E.P. Mitchell, Glycerol concentrations required for cryoprotection of 50 typical protein crystallization solutions, J. Appl. Crystallogr. 29 (1996) 584–587, https://doi.org/10.1107/S0021889896004190.
[22] P.R. Evans, G.N. Murshudov, How good are my data and what is the resolution? Acta Crystallogr. Sect. D Biol. Crystallogr. D69 (2013) 1204–1214, https://doi.org/10.1107/S0907444913000061.

[23] M.D. Winn, C.C. Ballard, K.D. Cowtan, E.J. Dodson, P. Emsley, P.R. Evans, R.M. Keegan, E.B. Krissinel, A.G.W. Leslie, A. McCoy, S.J. McNicholas, G.N. Murshudov, N.S. Pannu, E.A. Potterton, H.R. Powell, R.J. Read, A. Vagin, K.S. Wilson, Overview of the CCP4 suite and current developments, Acta Crystallogr. Sect. D Biol. Crystallogr. D 67 (2011) 235–242, https://doi.org/10.1107/S0907444910045749.
[24] T.C. Terwilliger, P.D. Adams, R.J. Read, A.J. Mccoy, N.W. Moriarty, R.W. Grosse-Kunstleve, P.V. Afonine, P.H. Zwart, L.-W. Hung, Decision-making in structure solution using Bayesian estimates of map quality: the PHENIX AutoSol wizard, Acta Crystallogr. Sect. D Biol. Crystallogr. D 65 (2009) 582–601, https://doi.org/10.1107/S0907444909012098.
[25] P.D. Adams, P.V. Afonine, G. Bunkóczi, V.B. Chen, I.W. Davis, N. Echols, J.J. Headd, L.W. Hung, G.J. Kapral, R.W. Grosse-Kunstleve, A.J. McCoy, N.W. Moriarty, R. Oeffner, R.J. Read, D.C. Richardson, J.S. Richardson, T.C. Terwilliger, P.H. Zwart, PHENIX: a comprehensive python-based system for macromolecular structure solution, Acta Crystallogr. Sect. D Biol. Crystallogr. D66 (2010) 213–221, https://doi.org/10.1107/S0907444909052925.
[26] P. Emsley, B. Lohkamp, W.G. Scott, K. Cowtan, Features and development of Coot, Acta Crystallogr. Sect. D Biol. Crystallogr. D 66 (2010) 486–501, https://doi.org/10.1107/S0907444910007493.
[27] G.N. Murshudov, P. Skubák, A.A. Lebedev, N.S. Pannu, R.A. Steiner, R.A. Nicholls, M.D. Winn, F. Long, A.A. Vagin, REFMAC5 for the refinement of macromolecular crystal structures, Acta Crystallogr. Sect. D Biol. Crystallogr. D 67 (2011) 355–367, https://doi.org/10.1107/S0907444911001314.
[28] A.J. McCoy, R.W. Grosse-Kunstleve, P.D. Adams, M.D. Winn, L.C. Storoni, R.J. Read, Phaser crystallographic software, J. Appl. Crystallogr. 40 (2007) 658–674, https://doi.org/10.1107/S0021889807021206.
[29] V.B. Chen, W.B. Arendall III, J.J. Headd, D.A. Keedy, R.M. Immormino, G.J. Kapral, L.W. Murray, J.S. Richardson, D.C. Richardson, MolProbity: all-atom structure validation for macromolecular crystallography, Acta Cryst. D 66 (2010) 12–21, https://doi.org/10.1107/S0907444909042073.
[30] The PyMOL Molecular Graphics System, Version 1.20 Schrodinger. , LLC, 2012.
[31] T.S. Chang, An updated review of tyrosinase inhibitors, Int. J. Mol. Sci. 10 (2009) 2440–2475, https://doi.org/10.3390/ijms10062440.
[32] A.D. Ryazanova, A.A. Alekseev, I.A. Slepneva, The phenylthiourea is a competitive inhibitor of the enzymatic oxidation of DOPA by phenoloxidase, J. Enzyme Inhib. Med. Chem. 27 (2012) 78–83, https://doi.org/10.3109/14756366.2011.576010.
[33] C. Eicken, F. Zippel, K. Büldt-Karentzopoulos, B. Krebs, Biochemical and spectroscopic characterization of catechol oxidase from sweet potatoes (Ipomoea batatas) containing a type-3 dicopper center, FEBS Lett. 436 (1998) 293–299, https://doi.org/10.1016/S0014-5793(98)01113-2.
[34] J. Poppe, J. Reichelt, W. Blankenfeldt, Pseudomonas aeruginosa pyoverdine maturation enzyme PvdP has a noncanonical domain architecture and affords insight into a new subclass of tyrosinases, J. Biol. Chem. (2018) 14926–14936, https://doi.org/10.1074/jbc.RA118.002560.
[35] X. Lai, H.J. Wichers, M. Soler-Lopez, B.W. Dijkstra, Structure and function of human tyrosinase and tyrosinase-related proteins, Chem. Eur. J. 24 (2018) 47–55, https://doi.org/10.1002/chem.201704410.
[36] T. Klabunde, C. Eicken, J.C. Sacchettini, B. Krebs, M.J. Henson, E.I. Solomon, Crystal structure of a plant catechol oxidase containing a dicopper center, Nat. Struct. Biol. 5 (1998) 1084–1090, https://doi.org/10.1038/4193.
[37] E.J. Drake, A.M. Gulick, Structural characterization and high-throughput screening of inhibitors of PvdQ, an NTN hydrolase involved in pyoverdine synthesis, ACS Chem. Biol. 6 (2011) 1277–1286, https://doi.org/10.1021/cb2002973.
[38] J.R. Theriault, J. Wurst, I. Jewett, L. Verplank, J.R. Perez, A.M. Gulick, E.J. Drake, M. Palmer, S. Moskowitz, N. Dasgupta, M.K. Brannon, S. Dandapani, B. Munoz, S. Schreiber, Identification of a small molecule inhibitor of Pseudomonas aeruginosa PvdQ acylase, an enzyme involved in siderophore pyoverdine synthesis, https://www.ncbi.nlm.nih.gov/books/NBK133446/#_ncbi_dlg_citbx_NBK133446 2013, Accessed date: 25 November 2019.
[39] K.D. Clevenger, R. Wu, J.A.V. Er, D. Liu, W. Fast, Rational design of a transition state analogue with picomolar affinity for Pseudomonas aeruginosa PvdQ, a siderophore biosynthetic enzyme, ACS Chem. Biol. 8 (2013) 2192–2200, https://doi.org/10.1021/cb400345h.
[40] D.R. Kirienko, D. Kang, N.V. Kirienko, Novel pyoverdine inhibitors mitigate Pseudomonas aeruginosa pathogenesis, Front. Microbiol. 9 (2019) 1–14, https://doi.org/10.3389/fmicb.2018.03317.
[41] S. Khan, M. Tareq Hassan Khan, M. Nadeem Kardar, Tyrosinase inhibitors from the fruits of Madhuca latifolia, Curr. Bioact. Compd. 10 (2014) 31–36, https://doi.org/10.1016/j.cell.2017.04.014.